How Does the W434F Mutation Block Current in *Shaker* Potassium Channels?

Youshan Yang, Yangyang Yan, and Fred J. Sigworth

From the Department of Cellular and Molecular Physiology, Yale University School of Medicine, New Haven, CT 06520

ABSTRACT The mutation W434F produces an apparently complete block of potassium current in *Shaker* channels expressed in *Xenopus* oocytes. Tandem tetrameric constructs containing one or two subunits with this mutation showed rapid inactivation, although the NH_2-terminal inactivation domain was absent from these constructs. The inactivation showed a selective dependence on external cations and was slowed by external TEA; these properties are characteristic of C-type inactivation. Inactivation was, however, incompletely relieved by hyperpolarization, suggesting the presence of a voltage-independent component. The hybrid channels had near-normal conductance and ion selectivity. Single-channel recordings from patches containing many W434F channels showed occasional channel openings, consistent with open probabilities of 10^{-5} or less. We conclude that the W434F mutation produces a channel that is predominantly found in an inactivated state.

KEY WORDS: ion channel gating • inactivation • mutation • patch clamp • potassium channels/physiology

INTRODUCTION

A tryptophan residue in the pore region of voltage-gated potassium channels, at position 434 of the *Shaker* B sequence, is highly conserved among the potassium channel subfamilies. Mutation of this residue to phenylalanine results in a *Shaker* channel with no measurable ionic current but essentially normal gating currents. Perozo et al. (1993) have demonstrated that in this mutant at least part of the channel gating machinery is intact, since intracellular tetraethylammonium (TEA) ions bind to the channel in a state-dependent manner, immobilizing the charge movement. Since in wild-type channels internal TEA appears to bind only when the channel is in the open state (Bezanilla et al., 1991; Perozo et al., 1992), it appears that the mutant channel undergoes the normal "closed-open" conformational change but nevertheless fails to conduct ionic current. Thus it would first appear that W434F mutation disrupts the ion permeation pathway. The 434 position is flanked by residues that have moderate effects on ion permeation (Yool and Schwarz, 1991; Kirsch et al., 1992); however, this position is relatively distant from the very sensitive positions 443-444 where mutations completely disrupt selectivity (Heginbotham et al., 1994). A cysteine residue at position 434 is accessible to the extracellular solution when probed with Ag^+ (Lü and Miller, 1995) but not when probed with methanesulfonate derivatives (Kürz et al., 1995), suggesting that the residue may be in a narrow part of the pore.

The W434F mutant has become a useful tool in biophysical measurements because it appears to completely eliminate ionic current through *Shaker* channels. Sigg et al. (1994) have exploited this property to record the small shot-noise fluctuations in gating currents. In similar recordings in our laboratory, we estimate that the fluctuations would have been contaminated were the single-channel conductance larger than about 10^{-3} of normal or if the channel open probability were greater than about 10^{-6} of normal. The present study attempts to shed some light on the mechanism by which this mutation so effectively eliminates the ionic current. In whole-cell and patch-clamp experiments on *Xenopus* oocytes we examine the properties of multimeric *Shaker* channels having one or two subunits containing the W434F mutation. We also examine some properties of the homomultimeric W434F channels.

MATERIALS AND METHODS

Tetramer Constructs

Constructs used in this study were based on a *Shaker* 29-4 construct, ShΔ, in which 30 amino acids at the NH_2 terminus were deleted to remove fast inactivation (Hoshi et al., 1990). *Shaker* 29-4 (Kamb et al., 1988) is identical to *Shaker* B (Schwarz et al., 1988) except in the NH_2-terminal alternatively spliced region and at four residues in the COOH-terminal region. The "wild type" tetrameric *Shaker* 29-4 construct WWWW (here W represents a "wild-type" protomer containing Trp at position 434) is made up of four concatenated ShΔ cDNAs with 19 amino acid linking regions (Lin et al., 1994; Fig. 1). Unique silent restriction sites engineered into the linker sequences facilitated the assembly of protomers into tandem constructs. The mutant constructs FWWW and FWFW (F represents a mutant protomer with Phe at position 434) were obtained by introducing the mutation into the first protomer, or first and third protomers, respectively, before assembly into the pGEM-A vector (Swanson et al., 1990).

Address correspondence to Dr. F.J. Sigworth, Department of Cellular and Molecular Physiology, Yale University, 333 Cedar Street, New Haven, CT 06520. E-mail: fred.sigworth@yale.edu

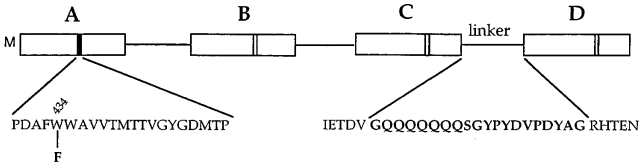

FIGURE 1. Diagram of the FWWW tetramer construct. Linkers 19 residues in length join four protomers, each consisting of the *Shaker* 29-4 sequence starting at residue 31. Each linker contains an HA epitope sequence. Protomer A contains an initial methionine residue preceding R31 and in this construct also contains the W434F mutation.

The mutations in protomer constructs were verified by sequencing, and assembly of the FWWW and FWFW constructs was verified by restriction mapping. Plasmids were linearized with NotI and cRNAs were transcribed with the MEGAscript T7 RNA polymerase kit (Ambion Inc., Austin, TX). Sizes of transcribed cRNAs were verified by gel electrophoresis.

Electrophysiology

The cRNAs of truncated *Shaker* 29-4 (ShΔ) and the tetrameric constructs were injected into *Xenopus* oocytes. Voltage-clamp and patch-clamp recordings were done at room temperature, 2–7 d after RNA injection. For two-microelectrode voltage clamp recordings, an OC-725 amplifier (Warner Instruments, Hamden, CT) was driven by the Pulse software (HEKA Electronic, Lambrecht, Germany) and an Instrutech (Mineola, NY) ITC-16 analog interface. Microelectrodes were filled with 1 M KCl and had 0.1–0.3 MΩ resistance. Patch clamp recordings were obtained using EPC-9 (HEKA Electronic) or Axopatch 200B (Axon Instruments, Foster City CA) amplifiers and pipettes pulled from 7052 glass (Corning Glass Works, Corning, NY).

The standard bath solution for voltage clamp recordings, denoted ND96, contained (in mM) 96 NaCl, 2 KCl, 1.8 $CaCl_2$, 1 $MgCl_2$, and 5 HEPES, pH 7.4. To test monovalent cation effects, Na^+ and K^+ were replaced completely by Rb^+, Cs^+, or K^+. To test effects of tetraethylammonium ion (TEA), 30 mM TEA-Cl replaced NaCl in the ND96 solution.

The bath solution for patch clamp recordings was (in mM): 140 K-aspartate, 1 KCl, 1 EGTA, and 10 HEPES, pH 7.4; unless otherwise noted the pipette solution was 5 K-aspartate, 135 Na-aspartate, 1.8 $CaCl_2$, and 10 HEPES, pH 7.4.

Half-amplitude threshold analysis (Colquhoun and Sigworth, 1995) was used to idealize single-channel recordings for dwell-time histograms and the reconstruction of ensemble time courses. Dwell-time histograms were fitted by maximum likelihood to mixtures of exponentials (Sigworth and Sine, 1987). Statistical quantities are expressed as mean ± SD with the number of determinations $n \geq 6$ in each case.

RESULTS

Accelerated Inactivation in Hybrid Channels

Whole-cell currents in oocytes injected with wild-type monomer and each tetrameric cRNA showed voltage-activated outward currents, with the main effect of one or two W434F mutations being the acceleration of inactivation (Fig. 2). Both the wild-type tetramer and the ShΔ channels showed slow inactivation with a time constant of about 5 s. Channels containing one or two W434F mutations inactivated much more rapidly, with prominent fast phases that decay in less than 1 s. Activation properties of these channel types, however, appeared to be unchanged, as shown by comparisons of the voltage dependence of peak conductance (Fig. 2 *E*). The voltage dependence of inactivation was however shifted by about −16 and −27 mV, respectively, when one or two mutant protomers were present. In addition to these effects, we observed that the peak current in FWWW- and FWFW-injected oocytes tended to be smaller, roughly 70 and 50% of the current observed in WWWW-injected oocytes.

To check for a change in channel selectivity, reversal potentials were measured in oocytes as they were bathed successively in the standard ND96 solution and in solutions containing 100 mM Cs^+, Rb^+, and K^+. Tail currents were measured under conditions chosen to minimize ion accumulation and inactivation; nevertheless the estimation of current reversal using the two-microelectrode voltage clamp, especially at potentials below −70 mV, can be subject to systematic errors due to the slow settling of the voltage clamp. However, a comparison of the apparent reversal potentials between WWWW and the mutant constructs shows that they are very similar (Table I). An exception is the case of external Rb^+, for which FWFW appeared to show a small but statistically significant decrease in relative permeability.

Effect of Extracellular Ions

Because N-type inactivation has been eliminated from our constructs through deletion of the NH_2-terminal "inactivation particle," the accelerated current decay in the mutant channels is likely to represent C-type inactivation (Hoshi et al., 1991). This inactivation process is modulated by extracellular cations and shows kinetic interactions with the block by extracellular TEA ions (Choi et al., 1991; Lopez-Barneo et al., 1993). We therefore tested the effects of external ions on the mutant channels. Increasing the extracellular potassium con-

TABLE I

Reversal Potential of Expressed Currents with Various External Solutions

Construct	ND96	100 Cs^+	100 Rb^+	100 K^+
WWWW	−70 ± 6.3	−58 ± 4.1	−0.83 ± 3.8	5.8 ± 3.8
FWWW	−72 ± 4.1	−57 ± 4.1	−3.3 ± 2.6	7.5 ± 2.7
FWFW	−69 ± 8.3	−55 ± 5.3	−7.5 ± 2.7	7.5 ± 3.8

Reversal potentials (in mV) were estimated from two-microelectrode voltage clamp recording from $n = 6$ oocytes in each case. After 5-ms activating pulses to +20 mV, tail currents were recorded during 10-ms test pulses to potentials between −80 and +20 mV. The tail current responses were interpolated to estimate the reversal potential. Pulses were delivered at 5-s intervals, the holding potential was −90 mV, and P/4 subtraction was employed.

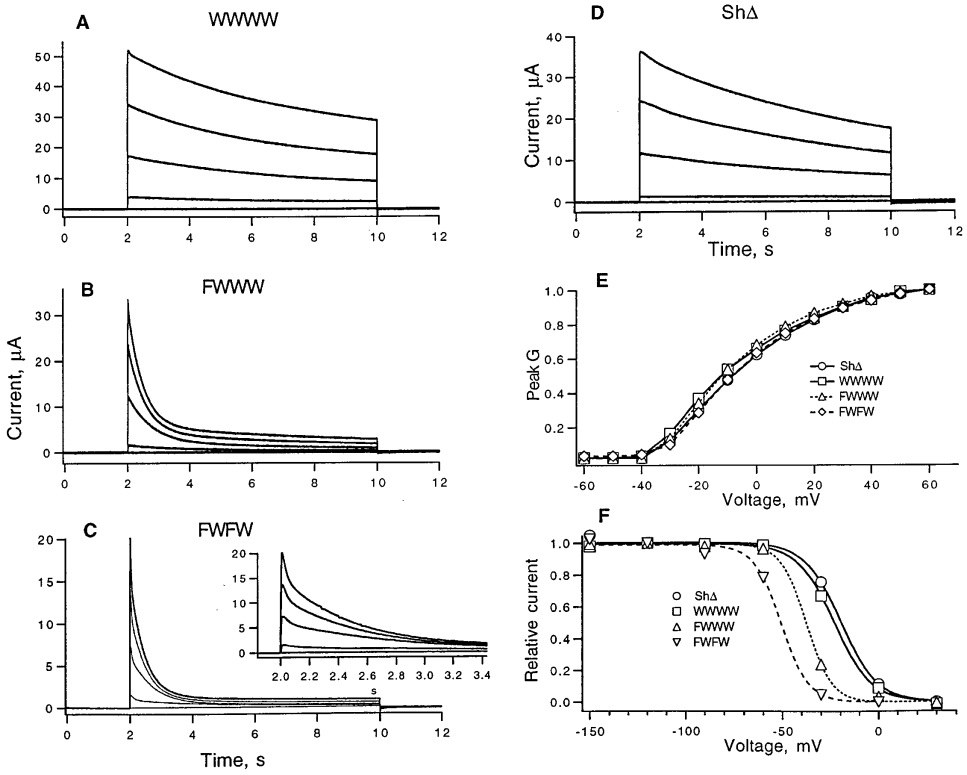

FIGURE 2. Ionic currents of *Shaker* wild-type, NH_2 terminus truncated monomer (*ShΔ*) and tetrameric constructs recorded with the two-microelectrode voltage clamp. (*A*) WWWW currents; (*B*) FWWW currents; (*C*) FWFW currents; (*D*) ShΔ currents; (*E*) peak G-V curves for the various channel types; (F) steady-state inactivation; the fitted curves are Boltzmann functions with midpoint voltages of −20, −23, −37, and −48 mV, and effective valences of 2.6, 2.6, 4.2, and 3.6 for ShΔ, WWWW, FWWW and FWFW, respectively. In each part of the figure, the holding potential was −90 mV, the bath solution was ND 96, and, except for the data plotted in *F*, leak currents were subtracted by the P/4 protocol (Bezanilla and Armstrong, 1977) with −120 mV leak holding potential. Depolarizing test potentials were from −50 to +30 mV in 20-mV steps in *A*, *B*, *C*, and *D*. Conductance in *E* was computed assuming a linear open-channel current-voltage relationship and a reversal potential of −85 mV. For the experiments in *F*, prepulses ranged from −150 to +30 mV in 30-mV steps and were 10 s in duration. They were followed by +30-mV depolarizing test pulse for 5 s; pulse sequences were delivered every 40 s, and leak current was subtracted using single P/4 pulses from a −140 mV leak holding potential.

centration had little effect[1] on the decay time course of WWWW currents, as measured during 8-s depolarizations to +40 mV (Fig. 3, *A* and *B*). In contrast, high K^+ had large effects on the time course of FWWW and FWFW currents. In each case fits to the decay required two exponential components. The effect of high K^+ was to slow the decay of the main component of FWWW currents or of both components in the case of FWFW.

There were also disparate effects on current amplitude. Increasing K^+ concentration reduced the peak current at +40 mV of WWWW channels, as would be expected as the reversal potential changes and the driving force is reduced for current through the channels (Fig. 3 *C*, *top*). For FWFW channels however there was a increase in current with K^+ concentration up to 20 mM; the current decreased when external K^+ was raised to 100 mM, but it was still larger than the current at 0.2 mM K^+ (Fig. 3 *C*, *bottom*). A similar effect, in which increasing external K^+ increases peak current, is observed in *Shaker* channels mutated at position 449 (Lopez-Barneo et al., 1993) and in a chimeric channel mutated at the position corresponding to 438 in *Shaker* (De Biasi et al., 1993).

The effect of external cations on inactivation of potassium channels has been shown to approximately follow the selectivity of ion permeation (Lopez-Barneo et al., 1993). We find that inactivation in FWWW and FWFW channels is most slowed with extracellular Rb^+ (Fig. 4 *A*) and follows the sequence $Rb \approx K > Cs > Na$ (Fig. 4 *B*). Like K^+, Rb^+ appears to increase the channel availability, allowing the currents in FWFW channels with 100 mM external Rb^+ to be as large as those in Cs^+ or Na^+, despite the reduced driving force at the test potential of +40 mV (Fig. 4 *C*).

Partial channel block by external TEA has been seen to be accompanied by a prolongation of the time course of C-type inactivation (Grissmer and Cahalan, 1989; Choi et al., 1991). In the presence of 30 mM TEA, a concentration near the K_d for the block of current in wild-type channels, a moderate slowing of the inactivation time course is seen in WWWW currents (Fig. 5 *A*). Slowing of the decay time courses is clearly seen in FWWW and FWFW currents (Fig. 5, *B* and *C*). Paradoxically, the peak FWFW current is also increased about 20% by the presence of 30 mM external TEA

[1]More rapid inactivation and a larger effect of external K^+ on wild-type channels was observed by Lopez-Barneo et al. (1993) in their recordings from outside-out patches. Although the small differences between the *Shaker* clones might be responsible, we suspect that the difference is likely due to extracellular ion accumulation in our whole-oocyte recordings.

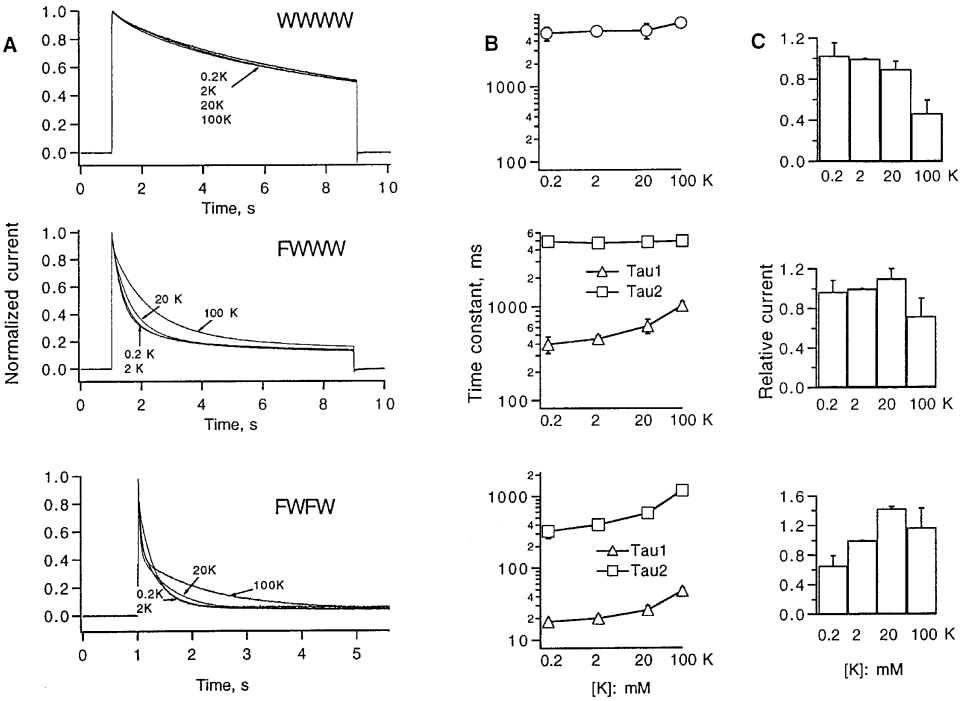

FIGURE 3. Effect of extracellular potassium on inactivation kinetics and peak currents of the three tetrameric constructs. (*A*) Normalized current time courses. Test pulses to +40 mV, 8-s duration were applied from a holding potential of −90 mV. The 2 mM K^+ bath solution was ND 96; the given K^+ concentration for the other solutions was obtained by replacing Na^+ with K^+. (*B*) Time constants of one (WWWW) or two (FWWW, FWFW) exponentials fitted to the inactivation time course at +40 mV. For FWWW the amplitude of the faster component was 73–82% of the total relaxation; for FWFW it ranged from 30 to 73% for the curves shown. (*C*) Relative peak currents at +40 mV in the various solutions normalized to the current in 2 mM K^+. Error bars in *B* and *C* represent standard deviations with $n = 6$ in each case.

(Fig. 5 *C*). This effect appears not to arise from shifts in the voltage dependence of activation or inactivation: 30 mM TEA caused only a small shift in the voltage dependence of peak conductance (Fig. 5 *D*), whereas voltage-dependent inactivation appears to be completely removed by the −90 mV holding potential used (Fig. 5 *E*). The kinetics of recovery from inactivation are also little changed by TEA or by high external K^+ (Fig. 5 *F*). Thus the current increase in the presence of TEA does not appear to result from a change in voltage-dependent parameters. Instead, it is likely that TEA binding affects the equilibrium of a voltage-independent pro-

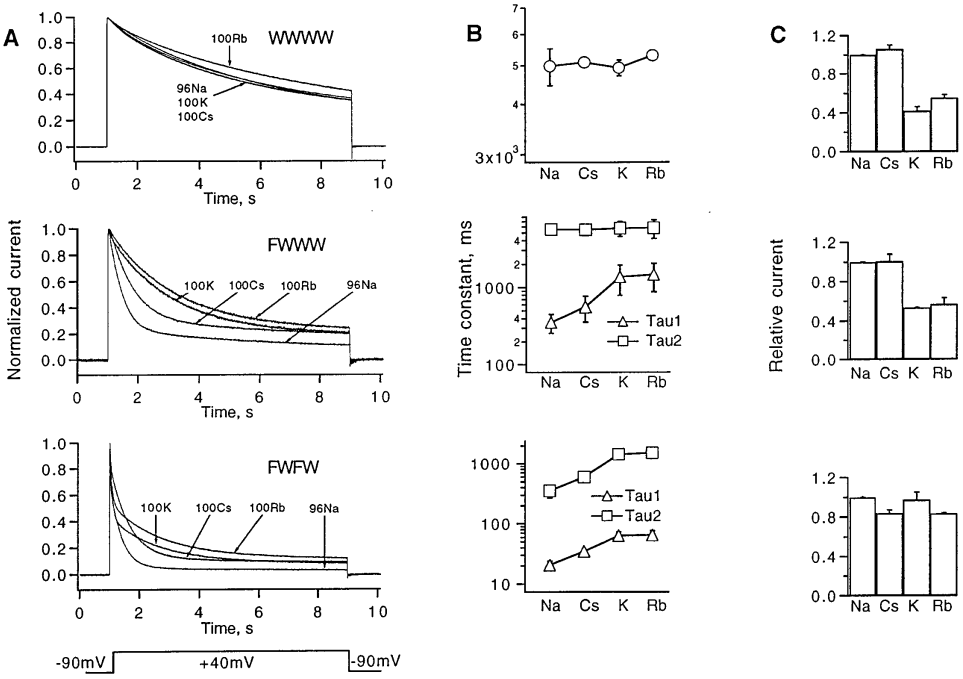

FIGURE 4. Effect of monovalent cations on inactivation kinetics and peak currents. (*A*) Normalized currents. Holding potential was −90 mV, test potential was +40 mV for 8 s. Cation concentrations are as indicated; 96Na refers to ND96 solution which contains 2 mM K^+. In the other solutions the indicated cation replaced both Na^+ and K^+. (*B*) Time constants from single or double-exponential fits to the decay time courses. (*C*) Relative peak currents in the various solutions normalized by current in the 96Na solution.

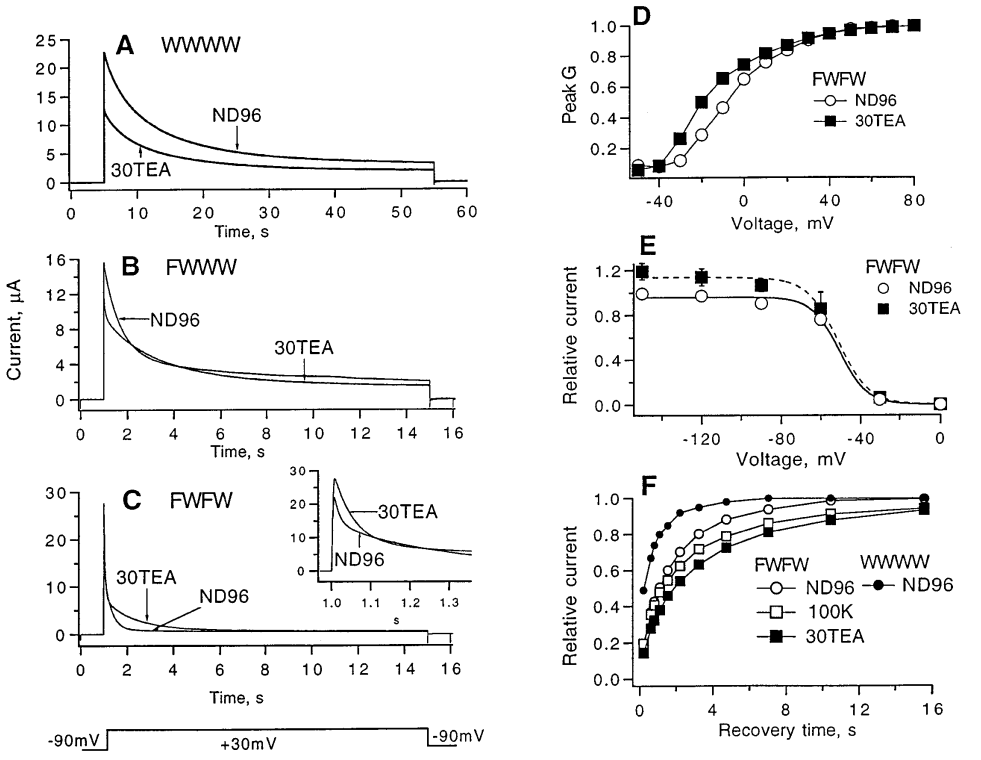

FIGURE 5. TEA effects on inactivation and activation. (*A*) Effect of 30 mM TEA in the bath solution (replacing Na^+ in ND96) on wild-type tetramer currents. Depolarizations to +30 mV were given for 50 s from a holding potential of −90 mV. The dissociation constant for channel block estimated under these conditions was 30 ± 7 mM (n = 14). (*B*) Currents from FWWW tetramers. External TEA slows the time course of inactivation. (*C*) FWFW tetramer currents. Inset shows the initial currents on an expanded time scale. (*D*) Voltage dependence of normalized peak conductance of FWFW in the absence and presence of 30 mM TEA. (*E*) Voltage dependence of FWFW inactivation in the absence and presence of 30 mM TEA. Prepulses of 10-s duration were followed by a +30-mV test pulse; the pulse sequence (including a single P/4 pattern) was repeated at 40-s intervals. From fits of Boltzmann functions the midpoint voltage and effective valence were −51 mV and 3.6 for FWFW currents in ND96, −51 mV and 3.2 in 30 TEA. (*F*) Time course of recovery from inactivation at −90 mV in the standard ND-96 solution or in external solutions containing 100 mM K^+ or 30 mM TEA. Plotted for FWFW is the peak current of a second depolarization to +30 mV, relative to that from an initial 5-s depolarization to +30 mV. For WWWW currents, which are incompletely inactivated by the 5-s prepulse, the fractional recovery (Levy and Deutsch, 1996) is plotted. Mean values for six experiments are shown in each case. "Recovery time" is the interval at −90 mV between the two depolarizations. Pulses were delivered at 60-s intervals.

cess that affects channel availability, as has been proposed to account for similar phenomena of "P-type" inactivation in the study of De Biasi et al. (1993).

Single-channel Recordings

We have fitted the time courses of inactivation in FWWW and FWFW channels with the sum of two exponentials. The slower of the two exponentials in FWFW currents has the same time constant as the predominant component in FWWW currents (see Fig. 3 *B*). This coincidence, coupled with reports that tandem multimeric constructs like ours do not entirely constrain the subunit content of expressed channels (McCormack et al., 1992; Hurst et al., 1995), suggests that multiple channel species might be present. To investigate this possibility, we made patch-clamp recordings from FWFW-injected oocytes. Two classes of activity were seen in patches containing a single channel. Out of 19 patches 12 showed rapid inactivation (Fig. 6 *A*), while 7 showed slower inactivation behavior (Fig. 6 *B*). A mixture of the two inactivation time courses describes well the currents observed in multi-channel patches (Fig. 6 *C*). The two components of inactivation show essentially no voltage dependence at depolarized potentials (Fig. 6 *D*). We conclude that the double-exponential decay of FWFW currents reflects two channel types. We shall assume that the rapidly inactivating channels as in Fig. 6 *A* contain two mutant subunits, i.e., are "true" FWFW channels, while the slowly inactivating channels of Fig. 6 *B* contain only one mutant subunit. Channels containing three mutant subunits would also be expected to be present. We did not observe a third population of channel activity, presumably because these channels would have a low open probability.

The FWFW single channel recordings show many blank sweeps (Fig. 6 *A*). Sweeps showing channel activity come in clusters of ~2 sweeps, separated by silent periods having a mean duration of about 4 sweeps (Fig. 7). The result is that a channel is available for opening only about one-third of the time. A runs test (Horn et al., 1984) shows that the grouping of channel activity is highly significant ($P < 0.002$), even in this experiment where pulses were delivered at 5-s intervals. Because of this low rate of "sampling" some brief dwells in states in which the channel is available (A) or unavailable (U) states are expected to be missed, but the pattern of activity is consistent with transitions between two states

$$\mathrm{A} \underset{0.05\ \mathrm{s}^{-1}}{\overset{0.1\ \mathrm{s}^{-1}}{\rightleftharpoons}} \mathrm{U} \qquad \text{(SCHEME 1)}$$

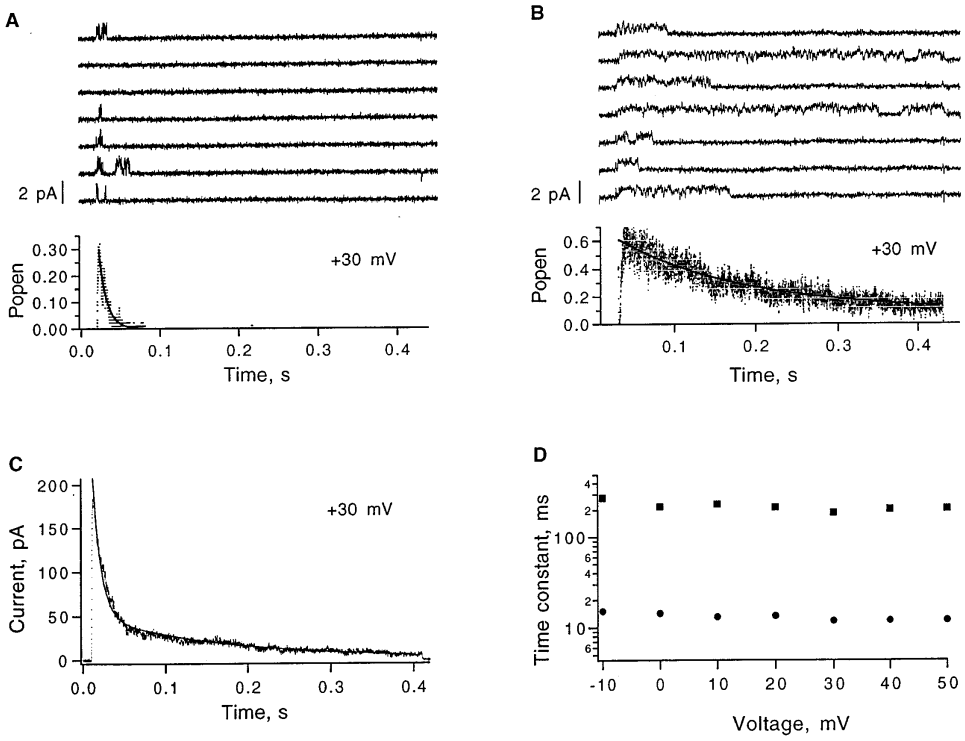

FIGURE 6. Inside-out patch recordings from FWFW-injected oocytes with the standard solutions (141 mM K^+ in the bath, 5 mM K^+ in the pipette). (*A*) Seven successive sweeps in a one-channel patch, showing bursts of openings in response to depolarization to +30 mV from −90 mV holding potential. Data were filtered at 2 kHz. The ensemble mean time course, obtained from 200 sweeps, shows a rapid decay from the maximum open probability of 0.3. The superimposed smooth curve is a single exponential with $\tau = 10$ ms. (*B*) Seven successive sweeps in a different one-channel patch show long bursts of openings in response to depolarizations to +30 mV from −90 mV holding potential. Filter bandwidth was 1 kHz. The ensemble mean time course, obtained from 100 sweeps, shows slow decay from an open probability of 0.6. The superimposed curve is a single exponential with $\tau = 150$ ms. (*C*) FWFW macroscopic current from a patch recording at +30 mV, filtered at 2 kHz. The superimposed smooth curve is the sum of two exponentials with time constants of 10 and 150 ms; the amplitudes of the components were 153 and 47 pA, respectively. (*D*) Time constants obtained in unconstrained, two-exponential fits to macroscopic currents at various potentials; same FWFW patch as in *C*. For single-channel recordings in *A* and *B*, leak subtraction used the average of null sweeps.

with the approximate rate constants given. The ShΔ and WWWW channel recordings also showed blank sweeps, but these occurred rarely, comprising only 2–3% of the total sweeps.

The single-channel conductance of FWFW channels is unchanged from wild type. Fig. 8 shows all-points amplitude histograms from ShΔ, WWWW, and FWFW single channel recordings. The FWFW histogram was accumulated from data filtered to 5 kHz bandwidth, because at the lower bandwidth used for the other histograms (2 kHz) the high rate of brief closures in FWFW channel currents caused obvious distortion of the histogram. The estimated slope conductances in the range 0 to +30 mV are near 13 pS for both wild-type and FWFW channels (Fig. 8 *B*).

The kinetics of FWFW single channels differ from the wild-type channels in several ways. FWFW channels have an increased prevalence of brief (~0.5 ms) closures. These closures occur about five times more frequently, shortening the mean open time from 2 to 0.4 ms (Fig. 9). In FWFW channel currents there is also a more prominent component of closed times having a time constant of 16 ms. These closures likely represent dwells in an intermediate state in a multistep inactivation process. This component is distinct from a third set of closures, the long closures that terminate the channel activity within 100 ms of the beginning of a depolarization (see Fig. 6 *A*).

Openings of Homomultimeric W434F Channels

We have seen that as one or two W434F mutations are incorporated into a *Shaker* channel tetramer, the single-channel conductance remains essentially the same but the gating properties change: the channel open time decreases, the probability of a channel opening in a sweep decreases, and the rate of inactivation increases. The acceleration of inactivation is seen to be partially opposed by the presence of high external K^+. Extrapolating to the case of four mutant subunits in a channel, one expects that homomultimeric mutant channels would have channel openings of normal amplitude, but these openings would be brief and rare. Such behavior is in fact seen. Occasional openings of W434F channels with 140 mM external K^+ are shown in Fig. 10. In this experiment the patch contained 2,400 channels, as computed from the magnitude of the gating current (Fig. 10 *A*). After subtraction of the mean time course from each sweep, single-channel events were detected in 164 of the 1,400 total sweeps. The peak open probability (Fig. 10 *C*) was seen to be 10^{-5}, and the channel activity showed an inactivation time constant

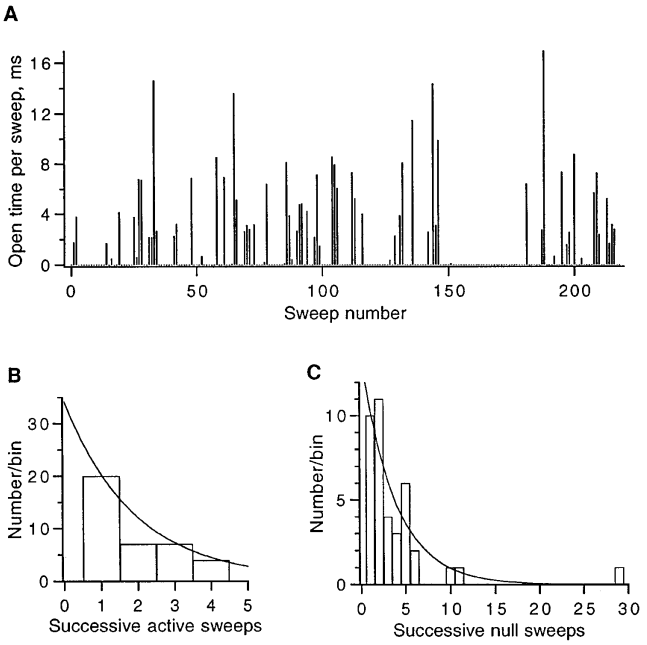

FIGURE 7. Activity of an FWFW single channel. (*A*) Diary plot showing the integrated open time in each of 220 depolarizations to +30 mV, 400-ms duration, delivered at 5-s intervals from a holding potential of −90 mV. Same patch as in Fig. 6 *A*. Of a total of 219 sweeps, 71 showed activity; the 69 runs of active and inactive sweeps is significantly ($P < 0.002$) smaller than the 97 runs expected for random activity. (*B*) Histogram of times in the "available" state. The mean dwell time was 1.9 sweeps; the superimposed curve represents a geometric distribution with this mean value. (*C*) Histogram of times in the "unavailable" state. The mean dwell time was 3.8 sweeps.

of 1 ms. The mean open time was 110 μs. In this experiment the contribution of ionic current to the total mean current is calculated to be 0.02 pA peak, much smaller than the 10.6 pA peak gating current.

The open probability of W434F channels is much lower in the absence of external K^+. In a patch recording like that in Fig. 10, but with *N*-methylglucamine replacing K^+ in the external solution, brief channel openings were detected in about 1% of sweeps from a patch containing 20,000 channels. The peak open probability in this case was less than 10^{-7}.

DISCUSSION

Evidence that channels with the W434F mutation do not simply have an occluded pore comes from a recent report by Starkus et al. (1997) that, in the absence of internal K^+, these channels conduct Na^+ ions but show anomalous gating. In the present study, we find that the W434F mutation, when present in one or two subunits of a tetrameric channel, enhances channel inactivation. The inactivation process shows the hallmarks of C-type or P-type inactivation, being selectively sensitive to external monovalent ions and being slowed by external TEA at a concentration that partially blocks the wild-type channel current. Unlike a classical voltage-dependent inactivation process, however, a substantial fraction of the channels remain unavailable for opening even when the holding potential is very negative. Patch recordings from homomultimeric mutant channels show rare channel openings, consistent with channels being predominantly inactivated.

Stoichiometry of the Expressed Channels

Tandem constructs containing two or four channel subunits have been successfully used in tests for cooperativity in gating and block of potassium channels (Heginbotham and MacKinnon, 1992; Hurst et al., 1992; Liman et al., 1992; Tytgat and Hess, 1992; Ogielska et al., 1995). However, the use of tandem cDNA constructs does not always guarantee that the channel protein assembles with the proper stoichiometry (McCormack et al., 1992; Hurst et al., 1995). Especially in the case of mutations

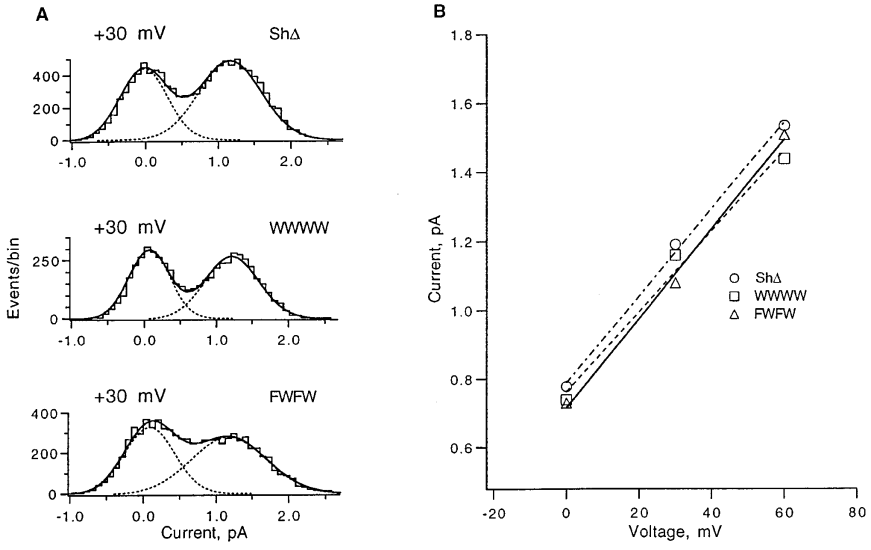

FIGURE 8. Single channel conductance of ShΔ, WWWW, and FWFW channels in the standard solutions. (*A*) Representative current amplitude histograms at +30 mV. For accumulation into all-points histograms, data were filtered at 2 kHz for ShΔ and WWWW, 5 kHz for FWFW. (*B*) Single channel current as a function of voltage obtained from double-Gaussian fits to amplitude histograms. Fitted lines have slopes of 13, 12, and 13 pS for ShΔ, WWWW, and FWFW respectively.

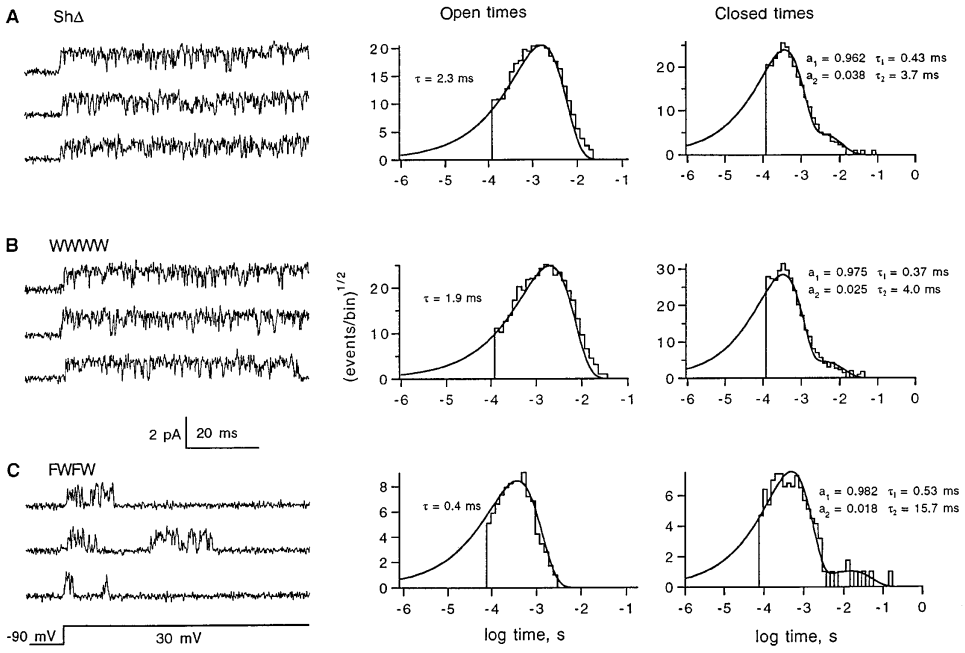

FIGURE 9. Open and closed time histograms from ShΔ, WWWW, and FWFW single-channel recordings. (*A*) Three successive sweeps from a one-channel recording of ShΔ and the corresponding open and closed time histograms. (*B*) WWWW currents. (*C*) FWFW currents. Data were filtered at 1.4 kHz for display and analysis in *A* and *B*, 2 kHz in *C*. Histograms contain more than 11,000 entries for ShΔ and WWWW, 630 entries for FWFW. Solid curves show maximum-likelihood fits of one exponential (*Open times*) or the mixture of two exponential distributions (*Closed times*).

that tend to reduce the level of expression, there appears to be the formation of multiple populations of channels. In the present study, the two phases of inactivation seen in FWFW-injected oocytes (Figs. 3 and 4) are readily explained if two populations of channels are present, each having a different rate of inactivation.

Single channel recordings (Fig. 6) do in fact show two types of channel behavior. Given the assumption that the majority of channels have the true stoichiometry of the tetrameric construct, we take the more rapidly decaying currents to reflect the true FWFW channels; the currents with a slower inactivation time course, one similar to that of macroscopic currents from FWWW-injected oocytes, we take to be from channels incorporating a single mutant subunit. Even if this assignment is not correct, the general conclusion of this study remains, that the inclusion of additional W434F subunits results in more rapid inactivation and a decrease in the steady-state availability of channels.

Voltage-independent Inactivation

Tetrameric constructs containing one or two mutant subunits yielded smaller currents than the WWWW construct when expressed in oocytes, and FWFW single channels were seen to open in only 30% of the sweeps recorded. The recordings in these cases were obtained with holding potentials sufficiently negative to remove voltage-dependent inactivation. The process causing "hibernation" of single FWFW channels, as modelled by the two-state SCHEME I, has a relaxation time constant of about 7 s. This is similar to the time constant of recovery from voltage-dependent inactivation in these channels (Fig. 5 *F*), suggesting a common mechanism for these phenomena. One such mechanism would consist of a voltage-independent, slow equilibrium between available and unavailable states that is coupled to channel activation similar, for example, to the allosteric model of Kuo and Bean (1994) for fast sodium channel inactivation. At rest the channel would undergo the transitions shown in the SCHEME I, while for an activated channel the equilibrium between available and unavailable states would be shifted more strongly toward the unavailable state.

A complete model for inactivation in FWFW channels would have to account not only for these slow transitions but also for inactivation transitions that occur on two more rapid time scales. The FWFW currents show an increased incidence of closures ~16-ms duration. These closures must represent dwells in states outside of the activation pathway, because the first latencies to channel opening are much shorter than this duration; thus it is likely that these closures represent dwells in a "pre-inactivated" state. The FWFW currents also show longer closures which terminate the channel activity during depolarizations. During 400-ms depolarizing pulses the channels never reopen from these longer closures. These longer closures cannot be the "unavailable" state of SCHEME I, however, because channels are seen to remain in the "available" state for several sweeps in succession (Fig. 7 *B*). In view of the multiple states that underlie these phenomena, our experiments do not provide enough kinetic information to construct a kinetic model for the inactivation process. We can only conclude that the inactivation process in FWFW channels is quite complicated.

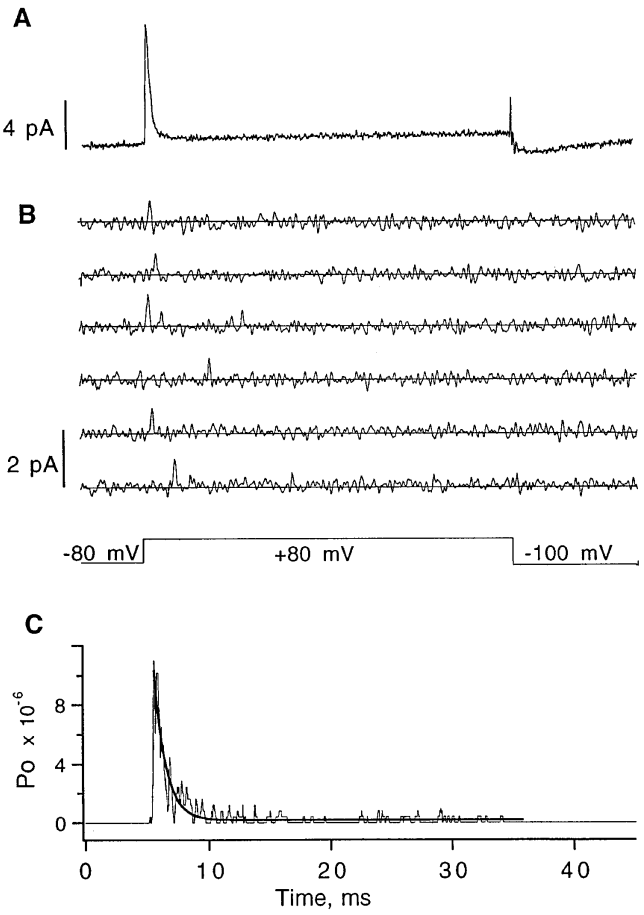

FIGURE 10. Cell-attached patch recording of W434F channels with 140 mM K^+ pipette solution. (*A*) Mean current (predominantly gating current) in response to depolarization to +80 mV from −80 mV holding potential; the average of 100 sweeps is shown. The patch contained 2,400 channels, as estimated from the integrated gating current assuming 13 e_0 of charge movement per channel. P/5 leak subtraction was used with a leak holding potential of −120 mV. (Contamination of gating current during the P/5 pulse produces the artifact preceding the "off" current.) Data were filtered at 5 kHz. (*B*) Six of the 164 sweeps with detectable ionic currents, selected from a total of 1,400 sweeps recorded. Data were filtered at 3 kHz and are displayed after subtraction of the mean of 100 sweeps to remove gating and leak currents. (*C*) Time course of open probability estimated from idealization of the sweeps containing channel activity. The superimposed curve is an exponential function with 1 ms time constant. The pipette solution contained (in mM) 140 K-aspartate, 1.8 $CaCl_2$, 10 HEPES, pH 7.4.

How Does W434F Block Ionic Current?

The term "C-type inactivation" was coined by Hoshi et al. (1991), who identified residues in the S6 region of *Shaker* COOH-terminal splice variants that affected the rate of residual inactivation remaining after NH_2-terminal truncation. Subsequent work has identified various mutations in the pore region that affect inactivation rate and channel availability in *Shaker*-channels (Pardo et al., 1992; Lopez-Barneo et al., 1993; Heginbotham et al., 1994; Yellen et al., 1994). Most of these authors, taking C-type inactivation to mean simply "the relatively slow inactivation process that remains in NH_2-terminal truncated channels," have ascribed their mutation effects to changes in this process. Thus over time the term C-type inactivation has become associated with a variety of phenomena. De Biasi et al. (1993) observed similar ion-dependent inactivation phenomena from a pore mutation of a Kv2.1-derived channel but observed also a paradoxical increase in channel current in the presence of external TEA; they ascribed the effect of this mutation, at a site corresponding to V439 in *Shaker*, to a distinct "P-type" inactivation process. We see a similar TEA effect in our FWFW hybrid channel. For the present discussion we shall nevertheless use the operational term "C-type inactivation" for all these phenomena, keeping in mind that it is quite possible that the ion dependence, voltage dependence, and TEA sensitivity could arise from distinct kinetic processes.

Our conclusion is that the W434F mutation almost completely eliminates the ionic current in *Shaker* channels by causing them to be permanently inactivated. C-type inactivation appears to be cooperative, in that individual subunits contribute to the energy barrier between the open and inactivated state (Ogielska et al., 1995; Panyi et al., 1995). Similarly, we observe increases in the rate of inactivation in going from zero to one to two subunits containing the W434F mutation in tetrameric channels, and an even more rapid current decay is seen in the rare single-channel events from W434F homotetrameric channels. The peak current through FWFW channels can be increased by extracellular K^+ or Rb^+, an effect associated with C-type inactivation that has been seen in various channel types and is influenced by mutations in the pore region (Pardo et al., 1992; De Biasi et al., 1993; Lopez-Barneo et al., 1993; Heginbotham et al., 1994). We find that the FWFW channels expressed in *Xenopus* oocytes have a substantial resting level of inactivation which cannot be removed by strong hyperpolarization. Also, channels containing four mutant subunits have a very low probability of being active, but their activity is greater in the presence of high external K^+.

If the W434F mutation yields channels that are permanently C-inactivated, a paradox arises in considering the observations of Roux et al. (1995). These authors observed a shift of the voltage dependence or "immobilization" of charge movement when long depolarizations were applied to W434F channels. The shift develops on a time scale of seconds, similar to the time course of C-type inactivation of ionic currents in channels lacking the W434F mutation, and similar to the time course of a shift or "charge immobilization" in native Kv1.5 channels (Fedida et al., 1996). The paradox is this: if mutant channels are already inactivated, how

can depolarization lead to a gradual change in charge movement, as would be expected from the development of inactivation? The answer to this question is not clear. One possibility is that there are multiple, independent inactivation processes, of which C-type is only one. Another possibility is that there is a single C-type inactivation process which is however sufficiently complicated to allow voltage-dependent processes to proceed in a channel that is already nonconducting by virtue of being in an inactivated state. We have presented evidence for the existence of several distinct inactivated states, consistent with either of these interpretations.

The W434F mutation is a very useful tool for biophysical studies, yielding channels having nearly normal gating currents but very small ionic currents. We find that the block of current in W434F channels is primarily a result of reduced open probability, not a reduction in permeability. The low probability of channel openings results in ionic currents that are negligible in comparison to the size of gating currents (Fig. 10). In measurements of gating-current fluctuations, however, the rare openings of "full sized" channels can make a substantial contribution to the measured variance, comparable in magnitude to the variance of the gating-current shot noise. To perform measurements of gating current fluctuations using these mutant channels it therefore will be necessary to further reduce the ionic current. The affinity for the channel-blocking toxin Agitoxin is reduced by the mutation (Aggarwal, 1996), but the use of impermeant ions to reduce the single-channel current should allow the variance of ionic currents to be made negligible.

We are grateful to L. Lin for the protomer constructs; to W.N. Joiner and R. Mathur for help with molecular biology; and J. Zheng and L. Islas for helpful discussions.

This work was supported by grant NS-21501 from the National Institutes of Health.

Original version received 30 January 1997 and accepted version received 10 April 1997.

REFERENCES

Aggarwal, S.K. 1996. Analysis of the voltage sensor in a voltage-activated potassium channel. Ph.D. Thesis, Harvard University. 80 pp.

Bezanilla, F., and C.M. Armstrong. 1977. Inactivation of the sodium channel. I. Sodium current experiments. *J. Gen. Physiol.* 70:549–566.

Bezanilla, F., E. Perozo, D.M. Papazian, and E. Stefani. 1991. Molecular basis of gating charge immobilization in *Shaker* potassium channels. *Science (Wash. DC).* 254:679–683.

Choi, K.L., R.W. Aldrich, and G. Yellen. 1991. Tetraethylammonium blockade distinguishes two inactivation mechanisms in voltage-activated K^+ channels. *Proc. Natl. Acad. Sci. USA.* 88:5092–5095.

Colquhoun, D., and F.J. Sigworth. 1995. Fitting and statistical analysis of single-channel records. *In* Single Channel Recording. 2nd ed. Plenum Press, New York. 483–587.

De Biasi, M., H.A. Hartmann, J.A. Drewe, M. Taglialatela, A.M. Brown, and G.E. Kirsch. 1993. Inactivation determined by a single site in K^+ pores. *Pflüg. Arch.* 422:354–363.

Fedida, D., R. Bouchard, and F.S.P. Chen. 1996. Slow gating charge immobilization in the human potassium channel Kv1.5 and its prevention by 4-aminopyridine. *J. Physiol. (Lond.).* 494:377–387.

Grissmer, S., and M. Cahalan. 1989. TEA prevents inactivation while blocking open K^+ channels in human T lymphocytes. *Biophys. J.* 55:203–206.

Heginbotham, L., Z. Lu, T. Abramson, and R. MacKinnon. 1994. Mutations in the K^+ channel signature sequence. *Biophys. J.* 66: 1061–1067.

Heginbotham, L., and R. MacKinnon. 1992. The aromatic binding site for tetraethylammonium ion in potassium channels. *Neuron.* 8:483–491.

Horn, R., C.A. Vandenberg, and K. Lange. 1984. Statistical analysis of single sodium channels. Effects of *N*-bromoacetamide. *Biophys. J.* 45:323–335.

Hoshi, T., W.N. Zagotta, and R.W. Aldrich. 1990. Biophysical and molecular mechanisms of *Shaker* potassium channel inactivation. *Science (Wash. DC).* 250:533–538.

Hoshi, T., W.N. Zagotta, and R.W. Aldrich. 1991. Two types of inactivation in *Shaker* K^+ channels: effects of alterations in the carboxy-terminal region. *Neuron.* 7:547–556.

Hurst, R.S., M.P. Kavanaugh, J. Yakel, J.P. Adelman, and R.A. North. 1992. Cooperative interactions among subunits of a voltage-dependent potassium channel. Evidence from expression of concatenated cDNAs. *J. Biol. Chem.* 267:23742–23745.

Hurst, R.S., R.A. North, and J.P. Adelman. 1995. Potassium channel assembly from concatenated subunits: effects of proline substitutions in S4 segments. *Receptors and Channels.* 3:263–272.

Kamb, A., J. Tseng-Crank, and M.A. Tanouye. 1988. Multiple products of the Drosophila *Shaker* gene may contribute to potassium channel diversity. *Neuron.* 1:421–430.

Kirsch, G.E., J.A. Drewe, M. Taglialatela, R.H. Joho, M. DeBiasi, H.A. Hartmann, and A.M. Brown. 1992. A single nonpolar residue in the deep pore of related K^+ channels acts as a K^+:Rb^+ conductance switch. *Biophys. J.* 62:136–143.

Kuo, C.C., and B.P. Bean. 1994. Na^+ channels must deactivate to recover from inactivation. *Neuron.* 12:819–829.

Kürz, L.L., R.D. Zühlke, H.-J. Zhang, and R.H. Joho. 1995. Side-chain accessibilities in the pore of a K^+ channel probed by sulfhydryl-specific reagents after cysteine-scanning mutagenesis. *Biophys. J.* 68:900–905.

Levy, D.I., and C. Deutsch. 1996. Recovery from C-type inactivation is modulated by extracellular potassium. *Biophys. J.* 70:798–805.

Liman, E.R., J. Tytgat, and P. Hess. 1992. Subunit stoichiometry of a mammalian K^+ channel determined by construction of multimeric cDNAs. *Neuron.* 9:861–871.

Lin, L., K. McCormack, and F.J. Sigworth. 1994. Subunit interactions in *Shaker* K^+ channel gating. *Biophys. J.* 66:106a.

Lopez-Barneo, J., T. Hoshi, S.H. Heinemann, and R.W. Aldrich. 1993. Effects of external cations and mutations in the pore region on C-type inactivation of *Shaker* potassium channels. *Receptors and Channels.* 1:61–71.

Lü, Q., and C. Miller. 1995. Silver as a probe of pore-forming residues in a potassium channel. *Science (Wash. DC).* 268:304–307.

McCormack, K., L. Lin, L.E. Iverson, M.A. Tanouye, and F.J. Sigworth. 1992. Tandem linkage of *Shaker* K^+ channel subunits does not ensure the stoichiometry of expressed channels. *Biophys. J.* 63:1406–1411.

Ogielska, E.M., W.N. Zagotta, T. Hoshi, S.H. Heinemann, J. Haab, and R.W. Aldrich. 1995. Cooperative subunit interactions in C-type inactivation of K channels. *Biophys. J.* 69:2449–2457.

Panyi, G., Z. Sheng, L. Tu, and C. Deutsch. 1995. C-type inactivation of a voltage-gated K^+ channel occurs by a cooperative mechanism. *Biophys. J.* 69:896–903.

Pardo, L.A., S.H. Heinemann, H. Terlau, U. Ludewig, C. Lorra, O. Pongs, and W. Stuhmer. 1992. Extracellular K^+ specifically modulates a rat brain K^+ channel. *Proc. Natl. Acad. Sci. USA.* 89:2466–2470.

Perozo, E., R. MacKinnon, F. Bezanilla, and E. Stefani. 1993. Gating currents from a nonconducting mutant reveal open-closed conformations in *Shaker* K^+ channels. *Neuron.* 11:353–358.

Perozo, E., D.M. Papazian, E. Stefani, and F. Bezanilla. 1992. Gating currents in *Shaker* K^+ channels. Implications for activation and inactivation models. *Biophys. J.* 62:160–168.

Roux, M.J., R. Olcese, L. Toro, and E. Stefani. 1995. Stabilization of the C-inactivated state by the fast inactivation particle in non-conducting *Shaker* H4 W434F potassium channels. *Biophys. J.* 68:A33.

Schwarz, T.L., B.L. Tempel, D.L. Papazian, Y.N. Jan, and L.Y. Jan. 1988. Multiple potassium-channel components are produced by alternative splicing at the *Shaker* locus of *Drosophila*. *Nature (Lond.).* 331:137–142.

Sigg, D., E. Stefani, and F. Bezanilla. 1994. Gating current noise produced by elementary transitions in *Shaker* potassium channels. *Science (Wash. DC).* 264:578–582.

Sigworth, F.J., and S.M. Sine. 1987. Data transformations for improved display and fitting of single-channel dwell time histograms. *Biophys. J.* 52:1047–1054.

Starkus, J.G., M.D. Rayner, and S.H. Heinemann. 1997. Anomalous conduction in the "non-conducting" *Shaker* K^+ channel mutant W434F. *Biophys. J.* 72:232a.

Swanson, R., J. Marshall, J.S. Smith, J.B. Williams, M.B. Boyle, K. Folander, C.J. Luneau, J. Antanavage, C. Oliva, S.A. Buhrow, et al. 1990. Cloning and expression of cDNA and genomic clones encoding three delayed rectifier potassium channels in rat brain. *Neuron.* 4:929–939.

Tytgat, J., and P. Hess. 1992. Evidence for cooperative interactions in potassium channel gating. *Nature (Lond.).* 359:420–423.

Yellen, G., D. Sodickson, T.Y. Chen, and M.E. Jurman. 1994. An engineered cysteine in the external mouth of a K^+ channel allows inactivation to be modulated by metal binding. *Biophys. J.* 66: 1068–1075.

Yool, A.J., and T.L. Schwarz. 1991. Alteration of ionic selectivity of a K^+ channel by mutation of the H5 region. *Nature (Lond.).* 349: 700–704.